

Biosynthesis and characterization of silver nanoparticles: A *Thymbraspicata*L extract approach and study their antibacterial and antifungal activity

Tayeb AB Matin^a, Nahid Ghasemi^{a,*}, Keivan Ghodrati^b, Majid Ramezani^a

^aDepartment of Chemistry, Arak Branch, Islamic Azad University, Arak, Iran

^bDepartment of Chemistry, Kermanshah Branch, Islamic Azad University, Kermanshah, Iran

Received: 12 May 2019, Accepted: 12 June 2019, Published: 1 November 2019

Abstract

In this study, at first, the biosynthesis of silver nanoparticles (Ag NPs) using an aqueous extract of *Thymbraspicata*L was studied and then, the shape and size of the synthesized NPs were characterized by different analysis such as UV-Vis, TEM, SEM, EDX, XRD, DLS and FT-IR. The synthesized Ag NPs were evaluated for their antibacterial activity against *Escherichia coli* (PTTC 1707), *Staphylococcus aureus* (PTTC 1112), *Bacillus cereus* (PTTC 1154) and *Aspergillus Niger* (PTTC 5012) and *Candida albicans* (PTTC5027) by a well-diffusion method and determination of minimum inhibitory concentration (MIC). Ag NPs displayed significant antimicrobial activity against the specimens, and they prevented the growth of bacteria and fungi at low concentrations.

Keywords: *Thymbraspicata*L; biosynthesis; silver nanoparticles; microbial activity; fungal activity.

Introduction

Nanotechnology refers to the design, characterization, production, and application of nanoscale structures and systems (1-100 nm) by controlling shape and size [1]. Conventional ways to produce NPs; including, chemical, physical, and biological methods have been used for many years [2]. There are many reports on the biological synthesis of Ag NPs using microorganisms such as bacteria, fungi, and plants; and all of them have shown antioxidant or reducing properties, which can reduce metal compounds [3].

Plants are an appropriate choice for green synthesis of NPs because of their

abundance and easy growth conditions and show many advantages over physical and chemical methods, and also are eco-friendly [4]. Use of plants for biosynthesis of NPs also has other advantages, *i.e.* it would be a complete reaction with low reaction time, production of uniform NPs with various shapes [5]. Silver NPs have shown size-dependent properties; including, optical, chemical, electrical, catalytic and antimicrobial properties, for this reason, it has been extensively studied [6]. Use biological methods lead to produce silver NPs with useful properties such as high surface area, small size, high

*Corresponding author: Nahid Ghasemi

Tel: +98 (86) 34135421, Fax: +98 (86) 34135421

E-mail: n-ghasemi@iau-arak.ac.ir, anahid3@gmail.com

dispersion, non-pathological, single-step and rapid procedures [7].

Silver has shown antimicrobial activity versus more than 650 microorganisms from different classes (such as gram-positive bacteria, gram-negative bacteria, fungi or viruses) [8]. Antimicrobial properties of silver NPs and its beneficial use in biotechnology and specific containment of microbes have been studied and proved in several studies, so that silver NPs can be effective in metabolism processes as well as the reproduction of microorganisms by inhibiting the respiratory system of bacteria [9] and also damage the bacterial cell membrane [10]. Several researches have proved the synthesis of silver NPs using plants [11]: Gardea *et al* reported the synthesis of silver NPs using plants for the first time with range sizes below 50 nm [12]. The synthesized silver NPs using garlic and *Pinus eldarica* with sizes of 10-40 and 20-30 nm respectively, showed good antimicrobial properties against some bacteria [13]. Antibacterial activity of AgNPs on gram-positive and gram-negative bacterial chain is not the same but one would have to follow other. There are conflicting reports of antibacterial activity against gram negative and gram positive. Some researchers have reported that gram-negative bacteria are more susceptible than the gram-positive bacteria to Ag NPs [14] and contradictory results are reported by other researchers [15]. Different sensitivity of both bacteria can be attributed to different structural properties of the species such as the shape and size of AgNPs, the amount of inoculated bacteria, time and nutrient medium used during the antibacterial activity analysis. The cell wall of gram-positive bacteria has peptidoglycan

molecule, and it has more peptidoglycan compared to the gram-negative bacteria. Because the cell wall of gram-positive bacteria is thicker and has negative charge, more positive silver ions penetrate into gram-positive bacteria by the peptidoglycan. Therefore, gram-positive bacteria are less susceptible that can be simply expressed by this fact that the cell wall in a gram-positive bacteria is thicker than gram negative. Antibacterial activity of AgNPs is relatively complicated and is not well-studied and its mechanism is only experimentally expressed. Antibacterial activity of AgNPs was divided into two categories: inhibitory activity and bactericidal activity. The previous strategy does not destroy the bacterial cells but can stop their division and subsequent bacterial cells will be destroyed due to the activity of AgNPs [16]. The mechanism of antibacterial activity of AgNPs is summarized in Figure 1. The graphical scheme in Figure 2 shows the result of bacterial growth filled with synthesized AgNPs using various green sources. The probable mechanism causes different behaviors in (a) to (e) which are shown on the right. In other words, a complete inhibitory activity close to the bactericidal activity with increasing concentrations of AgNPs is shown in Figure 2 [14b,17]. Experimental results support the morphological changes and perforation of the cell wall shown in Figure 2. The mechanism of bactericidal activity of AgNPs is shown through the release of Ag⁺ ions acting as a reservoir for antibacterial activity [14a]. The present study investigates the high potential of *Thymbraspicata* L extract in biosynthesis of silver NPs and their effects on several species of human pathogens and fungicides (Figure 3).

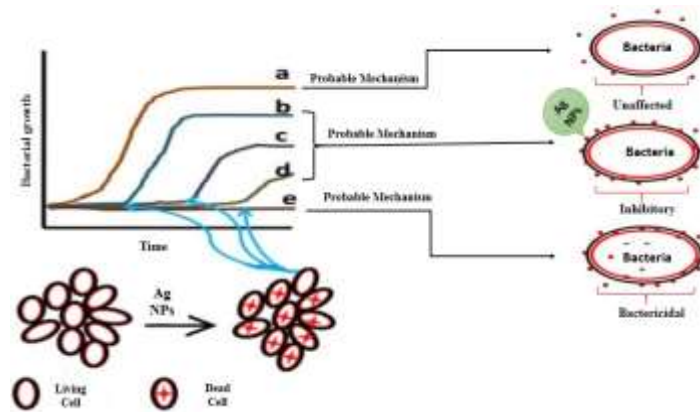


Figure 1. Mechanism of antibacterial action of Ag NPs

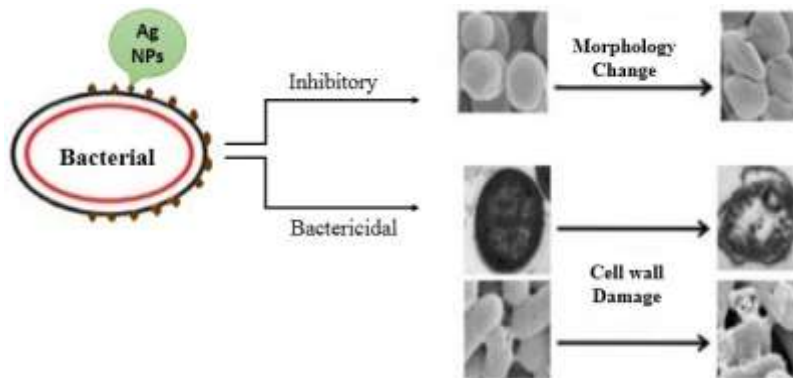


Figure 2. Morphological change and cell wall damage of bacterial cell

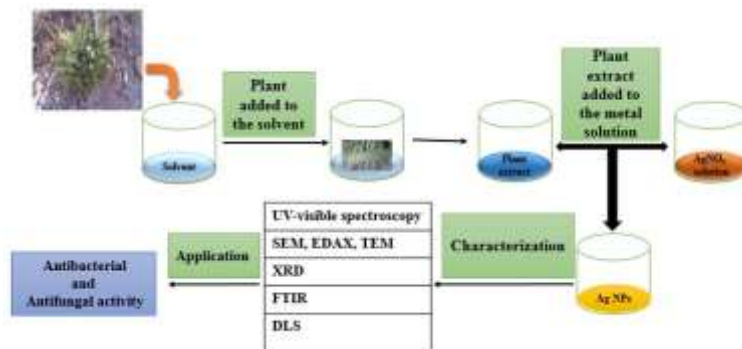


Figure 3. Biosynthesis of Ag NPs by *ThymbraspicataL* extract

Experimental

Chemical

Chemicals and microorganisms with high purity were used. Silver nitrate (AgNO_3) from Merck Co. (MERCK, Germany) and microorganisms; including, *Escherichia coli* (PTTC 1399), *Staphylococcus aureus* (PTTC 1112), *Bacillus cereus* (PTTC 1154),

Aspergillus (PTTC 5012) and *Candida albicans* (PTTC 5027) were purchased from Scientific and Industrial Research Organization of Iran (IROST). *ThymbraspicataL* is a plant of the *Lamiaceae* family, grows up to 40 cm height and can be collected from the city of Kermanshah in Kermanshah province. In addition, double distilled

water was used to prepare aqueous solution.

Preparation of Thymbraspicata extract

The fresh leaves were thoroughly cleaned with double distilled water and air dried at room temperature. Then, the dried parts were powdered by an electric mill. Afterwards, 1 g of powder was placed in a beaker containing 100 mL double distilled water for 30 min at 40°C in a water bath. The extract was cooled down to ambient temperature and filtered (Whatman filter paper no.42). To completely remove the suspended particles, the sample was centrifuged at 12,000 rpm for 10 min. In order to investigate the antimicrobial activity of the aqueous extract, 10 g of the powder was mixed with 100 mL distilled water and after 24 h, filtration procedure was carried out according to the previous step.

Initial synthesis of silver NPs

2 mL of the extract was added to 4 mL of 1 mM silver nitrate at laboratory temperature. It was observed that the color of the solution changed into brown indicating the formation of AgNPs. The effective parameters on AgNPs formations such as extract volume, silver ion concentration, reaction time and temperature were investigated. The formation of NPs was confirmed by UV-Visible spectroscopy.

Characterization of silver NPs

According to the existing research, the size and shape of NPs, as well as the efficiency of the NPs for antimicrobial properties depend on various factors such as extract volume, salt concentration, temperature and time. Several characterization techniques have been used to characterize the synthesized silver NPs under optimum conditions (for *Thymbraspicata* L extract: volume of extract: 2 mL;

concentration of silver nitrate: 1.5mM; temperature: 65°C; time: 60min); UV-Vis spectroscopy (Spectrophotometer Cary100), transmission electron microscopy (TEM) (Technai T20; Philips), X-Ray Diffraction (XRD) (Philips PW 1730), Dynamic light scattering (DLS) (Model: Nano S (red badg-632.8 nm)-Malvern UK Company), scanning electron microscopy (SEM) (TESCAN, Czech Republic), X-ray diffraction spectroscopy (EDX) (model: STADIP STOE Germany Company, and Fourier transform infrared (FT-IR) (Rayleigh WQF-327 510A spectrometer).

Antimicrobial activity investigation

Microbial samples were reduced based on standard methods using *Laura Bertani* and *Sabouraud Dextrose* Culture medium. In order to prepare microbial suspension, the 24-hour culture of each microorganism was separately inseminated to the test tubes containing 3 mL of *Mueller Hinton Broth* and, then, a suspension with the turbidity of 0.5 *McFarland* was obtained. Agar well-diffusion method (NCCLS 2006) was used to examine antimicrobial and antifungal effects of *Thymbraspicata* L extract. For this purpose, 100 µL of the suspension of each microbe was placed on a plate containing *Mueller Hinton* agar for bacteria and *Sabouraud Dextrose* agar for fungi and massively cultivated with a sterile swab in three directions. Then, at the surface of each cultivated plates, wells with a diameter of about 4 mm and a distance of 2.5 cm from each other were created and 70 µL of each dilution of the prepared aqueous extract were pipetted into each well. Antibacterial antibiotics like ampicillin and gentamicin and antifungal (clotrimazole) and DMSO were used as positive and negative control respectively. After that, bacterial

cultures were incubated at 37 °C for 24 h, and fungal cultures were incubated at 28 °C for 48 h, finally, after 24-48 h, microbial cultures were examined for the formation of the inhibition zone, and the diameter of the formed zones was measured (mm) and reported. Tube dilution method was used to specify the minimum inhibitory concentration (MIC) of the extract. For this purpose, different concentrations (1.25 mg/mL, 3.25 mg/mL, 25.6 mg/mL, 25.12 mg/mL, 25 mg/mL, 50 mg/mL, 100 mg/mL and 200 mg/mL) of the solution were prepared in 9 mL of *Mueller Hinton Broth* medium using the aqueous extract. Then, each tube was inoculated with 1 mL of the microbial suspension. A test tube containing the culture medium and inoculated microbe without extract as a positive control and a test tube containing the culture medium with the dilution of 25 mg/mL of extract without bacteria as a negative control were also prepared. Finally, all test tubes were incubated at 37 °C for bacteria and 28°C for fungi for 24-48 h. After incubation, each tube was examined for turbidity resulting from the growth of microorganisms and the lowest concentration that did not show any visible growth of microorganisms was determined as the MIC [18]. In order to investigate the antibacterial and antifungal effects of silver nanoparticles, well diffusion methods and MIC determination were used. The dilution series used to determine the inhibition growth of zone in well diffusion method (10, 20, 40, 60 and 100 µg/mL) and 50 µg/mL silver nitrate and gentamicin and clotrimazole were considered as a positive control. 10 test tubes with different dilutions of silver nanoparticles (220, 110, 55, 27.5, 13.75,

6.875, 3.4375, 1.7187, 0.8593, 0.4296 µg/mL) were used for each bacteria and fungi to determine Minimum inhibitory concentration (MIC). As a positive control, a tube containing only culture medium and inoculated microbes was used. For negative control and in order to ensure the sterilization of the process and the synthesized silver NPs suspension, one tube only containing culture medium and another tube containing culture medium and 0.5 µg/mL of silver NPs. Other steps of the work, such as preparation of culture medium, microbial strains, and the procedure have been similar to the methods in the experiment of aqueous extract of the plant.

Results and discussion

Optimization of effective parameters in silver NPs synthesis

In the initial synthesis of silver NPs using the aqueous plant leaves extract, the plant is considered as a reducing and stabilizing agent. Figure 4 shows the UV-Vis spectrum and the change in color of the silver NP solution without applying optimal conditions. According to Figure 4, there is not any peak for the extract around the surface plasmon resonance peak of the AgNPs at 430 nm, this suggests that the presence of the peak at this wavelength is due to the synthesis and presence of silver NPs, and the extract will not cause any possible interference with the spectrum of silver NPs. In order to study the effect of extract volume different volumes of (0.1, 0.2, 0.25, 0.5, 1, 1.5, 2.0 mL) the extract were added to 4 mL of 1 mM silver nitrate, then UV-visible spectroscopy was used to identify the optimum volume.

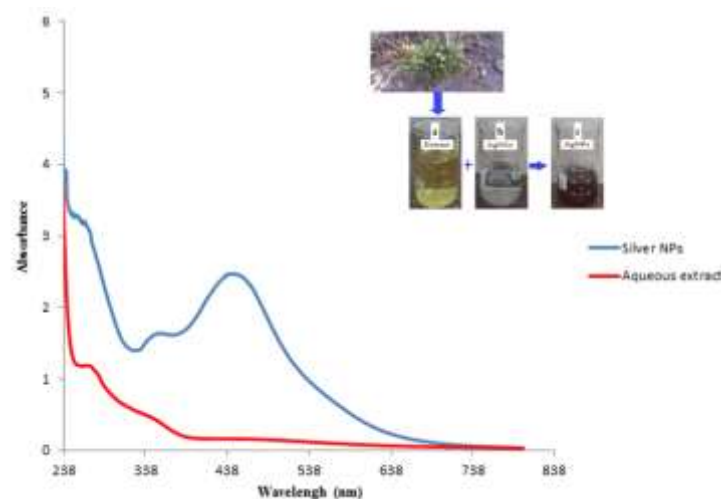


Figure 4. a) *ThymbraspicataL* herbal extract, b) 0.01 M silver nitrate solution, c) mixture of 0.01 M silver nitrate solution and *ThymbraspicataL* extract

As shown in Figure 5, the effect of surface plasmon resonance on UV spectrum is suitably observed and for all samples of *ThymbraspicataL* a sharp peak is observed at around 430 nm, the higher extract volume contains more concentration of *ThymbraspicataL* and, thus, on groups and molecules such as

tannins, phenols, alkaloids, and sugars, etc. So the absorption peak would be increased [19]. Thus, the reducing agents of silver ions and stabilizing agents of silver NPs would be increased. Finally, according to Figure 5, 2 mL was selected as the optimum volume of *ThymbraspicataL* extract.

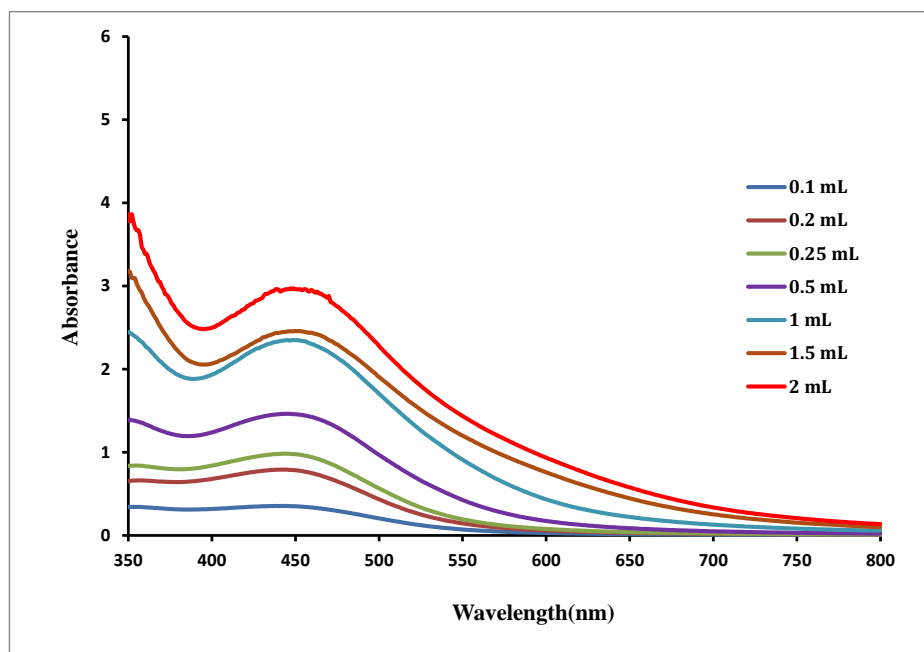


Figure 5. Influence of extract volume on silver NPs synthesis. (AgNO_3 (0.01mM) = 5 mL, $t=40\text{min}$, $T=\text{room temperature}$, stirring rate=150 rpm)

To investigate the effect of silver ion concentration, the optimized volume of the extract was added to 4 mL of different concentrations of (0.5, 1, 1.5, 2, 3, 5, 8 mM) silver nitrate. The optimum concentration was selected by measuring the UV–Vis spectrum of all solutions. Based on Figure 6, the results of the UV spectra for the effect of metal salt concentration indicate that by increasing the concentration of metal salts, surface plasmon resonance peaks for all samples appear at 430 nm, and smaller silver NPs with fewer size

dispersion will be obtained. Based on observations, the optimum concentration of silver nitrate was 1.5 mM for *Thymbraspicata*L extract. Some other experiments were performed (in an incubator shaker) under previous optimum conditions at different temperatures (25 °C, 35 °C, 45 °C, 55 °C, 65 °C, 75 °C and 85 °C) to attain the effect of the temperature change in silver NPs synthesis and the UV–Vis spectrum of all solutions was recorded and the optimum temperature was selected.

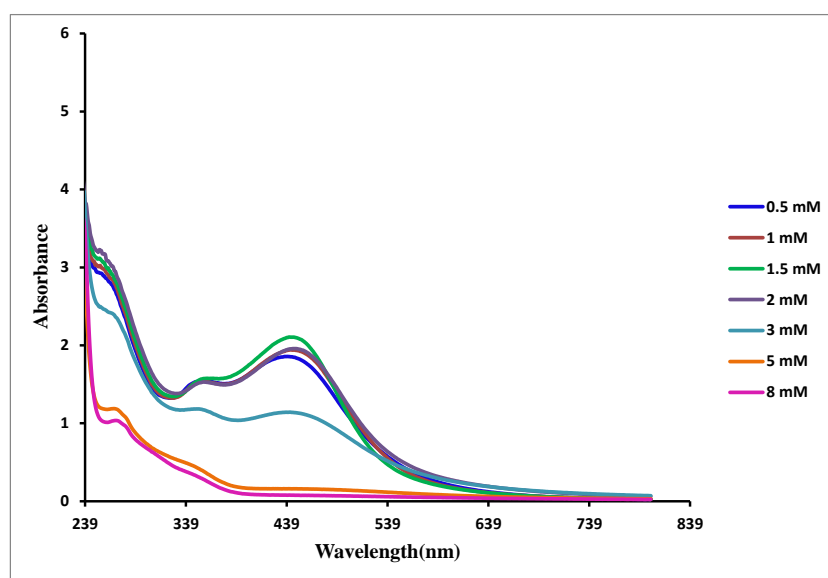


Figure 6. Influence of silver nitrate concentration on silver NPs synthesis. (Extract=2 μ l, t=40 min, T=room temperature, 150 rpm)

As seen in Figure 7, broad peaks around 475 nm are observed up to 45°C, that the peaks have become sharper and shift to 435 nm with increasing temperature, according to Figure 7, 65°C was chosen as the optimum temperature for silver NPs synthesis by *Thymbraspicata*L extract. However, an increase in temperature causes the alteration in the peaks due to the aggregation of NPs and eventually,

decreases the absorbance of nanoparticles. Similar results have been reported [20]. We also studied the effect of time in silver NPs synthesis, the solution was prepared under all previously optimized conditions at different times (10, 20, 30, 40, 50, 60, 120, 90 and 180 min), (From the instant of the reactants mixture to 3 h later). UV–Vis spectrum was measured for each, and the best time was selected.

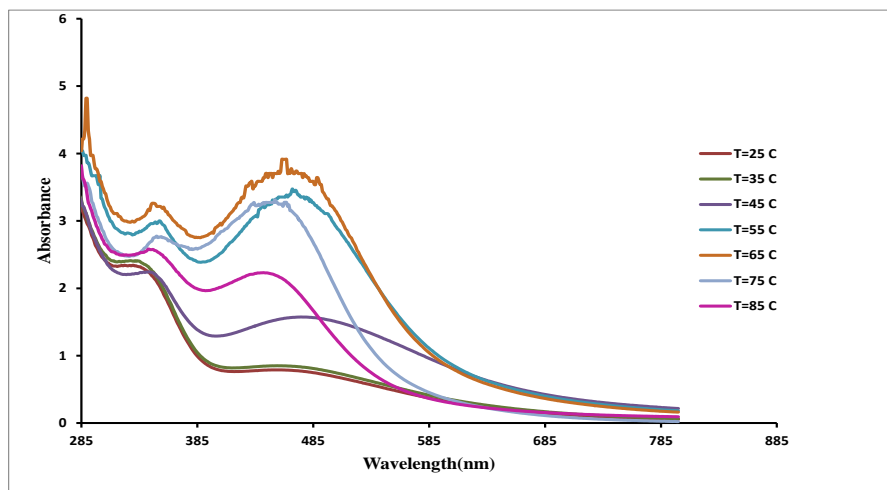


Figure 7. Influence of Temperature on silver NPs synthesis. ($C_{AgNO_3}=1.5$ mM, $V_{Extract}=2$ mL, $t=40$ min, 150 rpm)

Figure 8 shows the UV-Vis spectra related to the effect of time in the green synthesis of silver NPs using *ThymbraspicataL* extract. As can be seen, a small and weak peak appeared at 430 nm after 10 minutes from the beginning of the reaction, the sharpness of the peaks increased with increasing

time to 20, 30, 40, 50, 60, 120, 90 and 180 min, and after 60 min reaches to the maximum value at 430 nm, which is due to the significant formation of silver NPs. So, 60 min was chosen as the optimum time to improve the reaction [21].

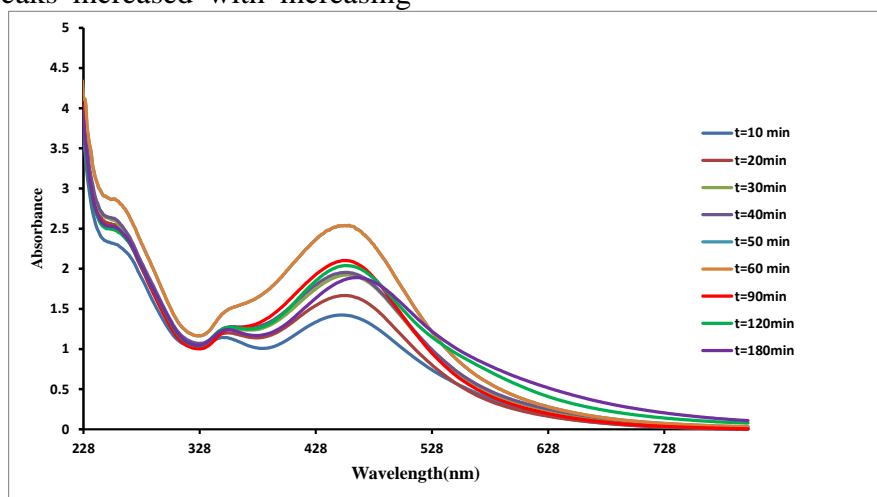


Figure 8. Influence of time on silver NPs synthesis. ($C_{AgNO_3}=1.5$ mM, $V_{Extract}=2$ mL, $T=60^{\circ}C$, 150 rpm)

Analysis of silver NPs with SEM and TEM analysis

The structure and surface morphology of silver NPs were characterized by scanning electron microscopy (SEM). SEM image clearly confirmed the

presence of cubic silver NPs with the sizes between 2.7 to 47 nm (Figure 9) and the average size of 20 nm. SEM results are very similar to reports of other researchers [22]. The size of the synthesized NPs was analyzed using

transmission electron microscopy (TEM), operating at an accelerating voltage of 200 kV. Before the measurements, the aqueous suspension of NPs was placed on carbon-coated copper grids and allowed to dry. Figure 10 shows the TEM image of the

synthesized silver NPs by applying all optimized conditions. According to the TEM result, silver NPs using *ThymbraspicataL* extract having face-centered cubic (fcc) structure with the average particle size of 20 nm which is same with SEM analysis.

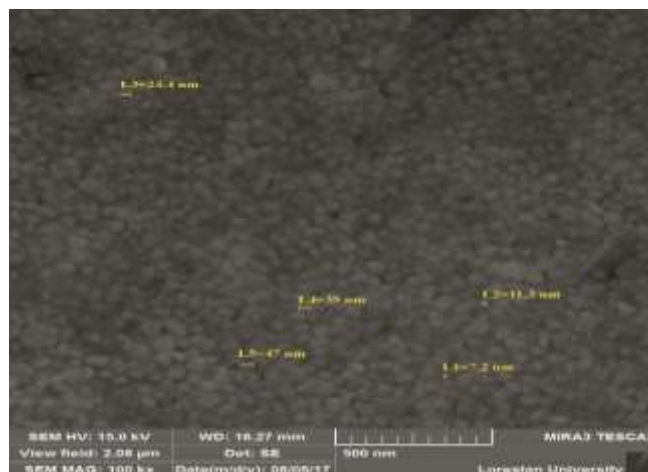


Figure 9. SEM image of AgNPs using *ThymbraspicataL* extract

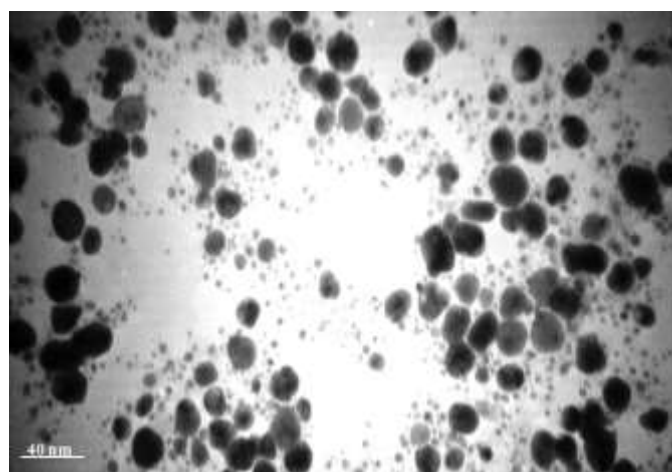


Figure 10. TEM image of AgNPs using *ThymbraspicataL* extract

Analysis of silver NPs with EDX

Energy-dispersive X-ray spectroscopy is used to show elemental analysis or chemical characterization of a sample. It is an elemental analysis that can be represented as a linear elemental analysis (on a hypothetical line in SEM image) or an elemental mapping (dispersion of the elements in the image). The EDX spectrum confirmed

the presence of carbon, nitrogen, chlorine and silver in the synthesized Ag-NPs (Figure 11). The EDX analysis verified that the NPs contained a large amount of Ag: 60.20 atomic %, C: 24.68 atomic %, N: 12.81 atomic % and Cl 2.31 atomic %, which C, N and Cl originated from the plant extract (Quantitative results are presented in Table 1). The presence of Ag indicated

the formation of silver NPs. The existence of C, N and Cl in the EDX spectrum can be related to the presence of biomolecules on the surface of the silver NPs [23], as indicated in the synthesis of gold NPs [24]. As shown in Figure 11, the presence of silver

particles and carbon atoms is significant, which is in good agreement with the purpose of this study. The EDX analysis reveals a strong signal at 3 keV which is generally shown by metallic silver nano-crystals due to surface plasmon resonance [25].

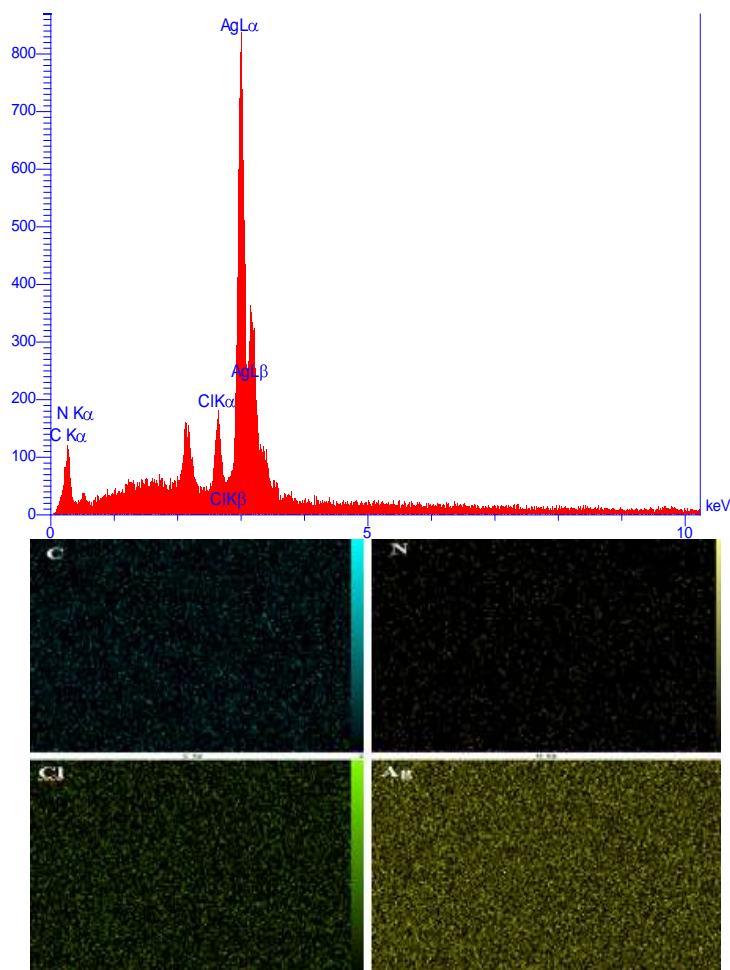


Figure 11. EDX image and elemental mapping of Ag NPs

Table 1. Quantitative results of EDX analysis of the synthesized silver NPs using ThymbraspicataL

Elt	Line	Int	Error	K	Kr	W%	A%	ZAF	Pk/Bg	LConf	HConf
C	Ka	31.6	3.1496	0.1640	0.1155	24.68	57.19	0.4681	12.48	23.44	25.92
N	Ka	5.8	3.1496	0.0391	0.0276	12.81		0.2153	7.11	11.31	14.31
Cl	Ka	40.6	1.7537	0.0317	0.0223	2.31	1.82	0.9636	5.82	2.21	2.42
Ag	La	414.4	1.7537	0.7652	25.45	60.20	15.54	0.8951	29.84	59.37	61.04

XRD analysis

X-ray diffraction analysis was used to study the crystalline structure of the

synthesized AgNPs. The sample for XRD analysis was prepared by depositing the centrifuged sample on

amicroscopic glass slide and air-dried overnight. The diffractogram was recorded in a PAN analytical, XPERT-PRO diffractometer using Cu K α ($\lambda = 1.54060 \text{ \AA}$) as an X-ray source. As shown in Figure 12, the lattice planes (111), (200), (220) and (311), which corresponded to diffraction peaks at 38.31, 44.40, 64.68, and 77.69, clearly confirmed that the geometric shape of the synthesized NPs is face-centered cubic (fcc) [26]. The presence of sharp peaks in the pattern indicated a high degree of crystallinity for silver NPs.

The crystal size of the Ag crystallites is calculated from the peak widths using the Scherrer-Debye equation (Eq. 1) (Table 2):

$$D = 0.9\lambda / \beta \cos\Theta \quad (1)$$

Where D is the average size of crystalline grains, β : full width at half maximum, λ : the wavelength of the x-rays. The estimated average size of the synthesized crystalline grains is 31.21 nm by Debye-Scherrer equation which is in an agreement with the results of the transmission electron microscopy and UV-Vis spectra.

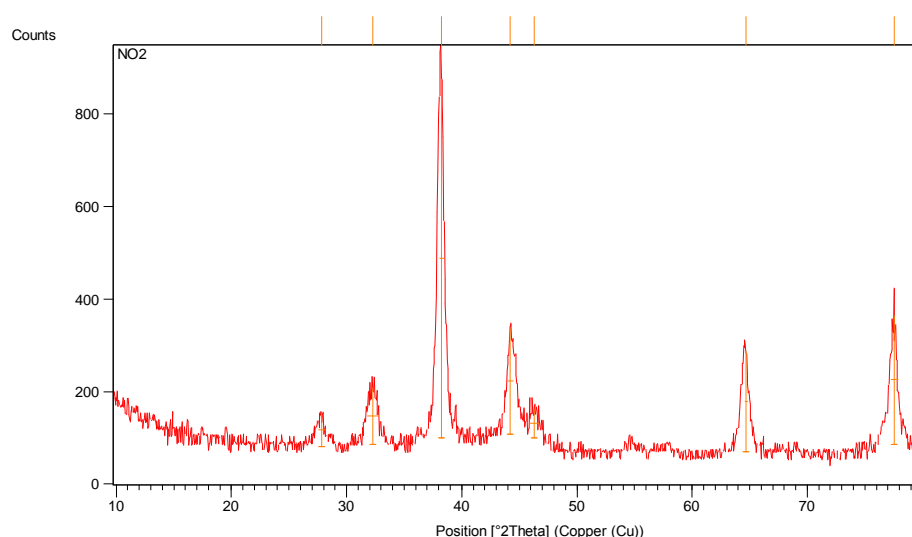


Figure 12. XRD image of AgNPs using *ThymbraspicataL* extract

Table 2. Precise details for calculating silver NP size

NO	Pos. [°2Th.]	FWHM [°2Th.]	hkl	d-spacing [Å]	Size (nm)
1	38.306540	0.246000	111	2.34973	32.38
2	44.396340	0.787200	200	2.04054	11
3	64.685940	0.590400	220	1.44104	15.93
4	77.689860	0.393600	311	1.22914	25.95
					Ave.=21.3

FT-IR analysis

For the FT-IR analysis, the vacuum-dried NPs were mixed with potassium bromide (KBr) and the spectra were recorded in the 4000–400 cm^{-1} range with the resolution of 4 cm^{-1} . The functional groups that are responsible for the biosynthesis of silver NPs are identified by FT-IR analysis. The FT-IR

spectrum of *ThymbraspicataL* extract (before reaction with AgNO_3) and the synthesized silver NPs using the extract (after reaction with AgNO_3) are shown in Figure 13. It can be seen that both FT-IR spectrums showed a change in the following peaks: 3414–3413 cm^{-1} (corresponding to the OH stretching of phenol and carboxylic acid), 2923–

2924 cm^{-1} (due to C-H stretching), 1618-1616 cm^{-1} (due to C=C stretching), 1070-1051 cm^{-1} (can be assigned to the phenolic compounds C-O). In addition, the peak at 1637 cm^{-1} is attributed to the

carbonyl stretch (C=O) contained in *Thymbraspicata* extract, but this peak does not exist in the synthesized silver NPs.

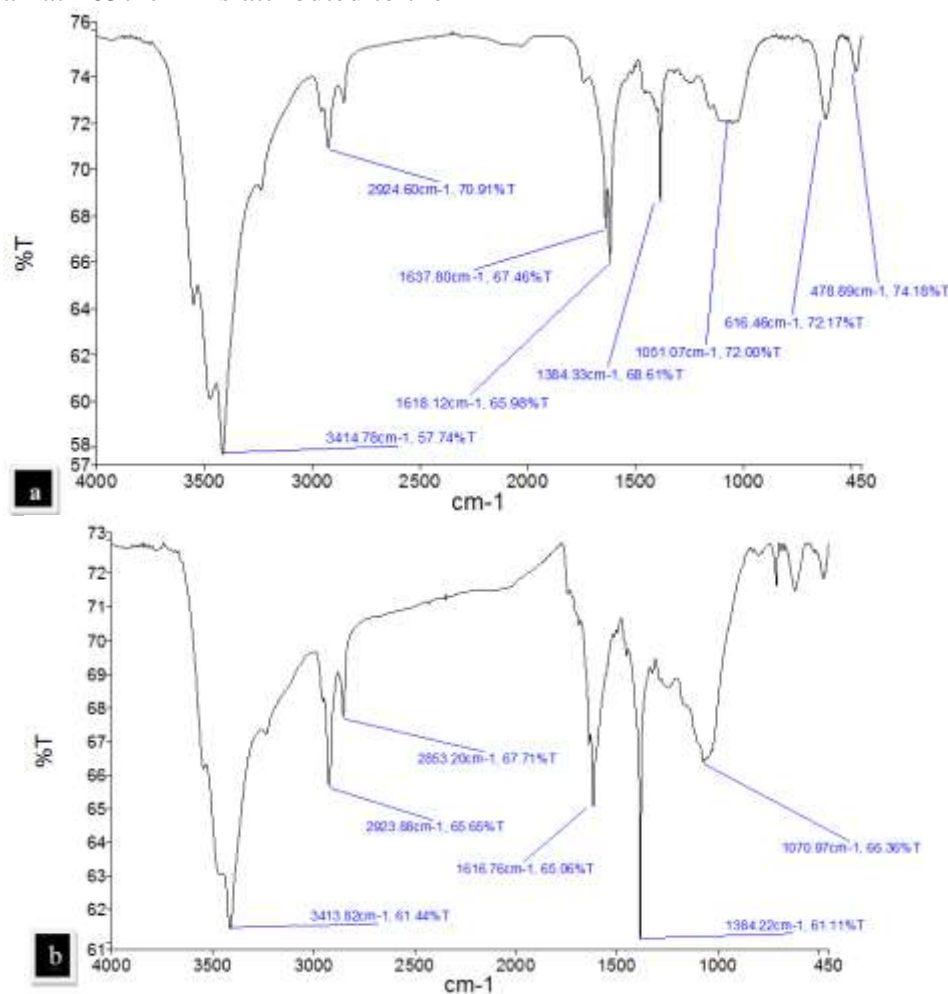


Figure 13. FT-IR spectra of a) ThymbraspicataL and b) Ag NPs synthesized from the peel extract

DLS analysis

Dynamic light scattering (DLS) was used to analyze the particle size distribution. The light scattering technique of the synthesized NPs was observed using Malvern Zetasizer Version 6.20. The mean size of particles recorded by DLS is 36.8 nm (Figure 14). The obtained size from DLS measurement is larger than the result of TEM. The differences, possibly due to the detection of small amounts of large

particles measured by agglomer or contamination, causes uncertainty in the particle size. Significant differences in both analyses probably indicate that TEM only measures a number based size distribution of the physical size and does not include any capping agent, while DLS measures the hydrodynamic diameter (particle diameter), and also molecules or ions that are attached to the surface and moves with the AgNPs in solution.

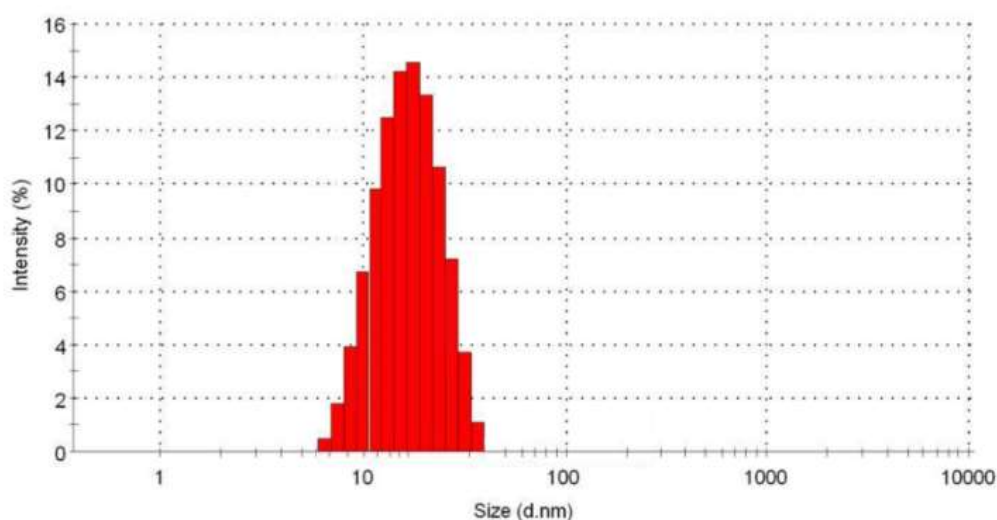


Figure 14. Diagram of treated silver NPs size distribution with ThymbraspicataL extract

Antimicrobial activity of ThymbraspicataL extract

The results of antimicrobial and anti-fungal effects of the aqueous extract of *ThymbraspicataL* showed that the extract has a significant inhibitory effect on all bacteria and fungi, in which the diameter of the inhibition zone and inhibitory effect would be increased with increase in concentration. The results of the different concentrations effects of *ThymbraspicataL* aqueous extract by well-diffusion method are shown in Table 3. The sensitivity of

gram-positive bacteria compared to gram-negative bacteria and fungi is clear. The results of the minimum inhibitory concentration (MIC) of the aqueous extract against the selected microbes by tube dilution method are shown in Table 4. Among bacteria, *Staphylococcus aureus* (MIC 14.4) and among fungi, *Candida albicans* (MIC 7.2) showed the highest sensitivity and *Pseudomonas aeruginosa* (MIC 115.2) showed the lowest sensitivity to the extract (Figure 15).

Table 3. Diameter of inhibition zone at different concentrations of Thymbraspicata L. aqueous extract by diffusion method (mL)

Microorganism	Different concentrations of aqueous extract(mg/mL)					Ampicillin	Clotrimazole	DMSO
	25	50	100	200	400			
Candida albicans	8	9	12	14	17	-	26	0
Pseudomonas aeruginosa	0	6	8	12	13	22	-	0
Aspergillus	8	10	12	15	18	-	24	0
Escherichia coli	6	7	10	12	14	23	-	0
Bacillus cereus	7	9	12	15	23	24	-	0
Staphylococcus aureus	8	9	11	14	17	22	-	0

Table 4. Minimum inhibitory concentration of Microbial Growth (MIC) at different concentrations of Thyme Spicata L aqueous extract

Microorganism	Different concentrations of aqueous extract(mg/mL)							
	1.8	3.6	7.2	14.4	28.8	57.6	115.2	230.4
Candida albicans	+	+	-	-	-	-	-	-
Pseudomonas aeruginosa	+	+	+	+	+	+	-	-
Aspergillus	+	+	+	-	-	-	-	-
Escherichia coli	+	+	+	+	+	-	-	-
Bacillus cereus	+	+	+	+	-	-	-	-
Staphylococcus aureus	+	+	+	-	-	-	-	-

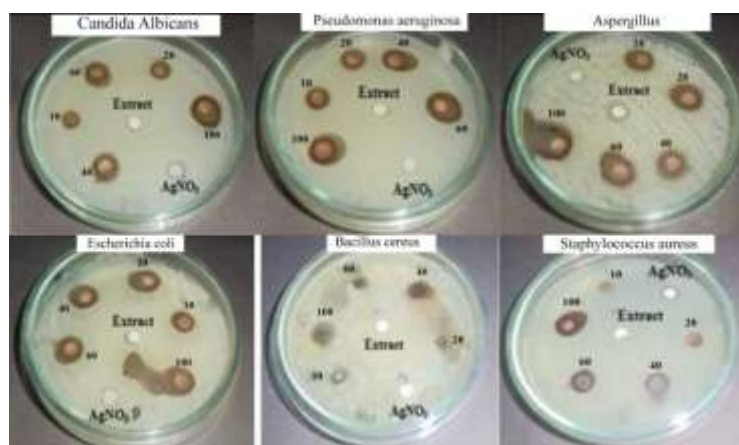


Figure 15. Antibacterial and anti-fungal properties of silver NPs synthesized with medicinal plant extract *ThymbraspicataL* at concentrations (10, 20, 40, 60 and 100 mg/mL), Nitrate silver solution (1.5 mM), Plant extract *ThymbraspicataL*

Antimicrobial activity of synthesized silver NPs using ThymbraspicataL extract

The results of the antimicrobial tests for the synthesized silver NPs by diffusion methods and MIC determination are presented in Table 5 and Table 6, respectively. The synthesized NPs showed significant antimicrobial effects on the samples, so at very low concentrations prevented the growth of bacteria and fungi, and while the aqueous extract of the plant at those

concentrations did not show any antimicrobial activity, the antimicrobial activity of silver was also much lower than silver NPs. Based on the results, AgNPs showed the greatest inhibition against *Escherichia coli* (zone diameter = 21 mm and MIC = 3.6 µg/mL) and *Aspergillus Niger* (zone diameter = 20 mm and MIC = 3.6 µg/mL) and the least inhibition against *Staphylococcus aureus* bacteria (zone diameter = 16 mm and MIC = 38.8 µg/mL).

Table 5. The inhibition zone diameter at different concentrations of silver NPs by well diffusion method (mL)

Microorganism	Different concentrations of aqueous extract(mg/mL)						Silver salt solution (50 µg/mL)	Clotrimazole (50 µg/mL)
	10	20	40	60	100			
Candida albicans	8	10	13	16	19		10	24
Pseudomonas aeruginosa	7	10	12	16	19		10	-
Aspergillus	8	11	14	17	20		9	25
Escherichia coli	8	10	13	16	21		11	-
Bacillus cereus	6	8	10	13	17		8	-
Staphylococcus aureus	0	6	11	13	16		7	-

Table 6. Minimum inhibitory concentration (MIC) at different concentrations of silver NPs (µg/mL)

Microorganism	Different concentrations of aqueous extract(mg/mL)										
	0.45	0.9	1.8	3.6	7.2	14.4	28.8	57.6	115.2	230.4	460.8
Candida albicans	+	+	+	+	-	-	-	-	-	-	-
Pseudomonas aeruginosa	+	+	+	+	-	-	-	-	-	-	-
Aspergillus	+	+	+	-	-	-	-	-	-	-	-
Escherichia coli	+	+	+	-	-	-	-	-	-	-	-
Bacillus cereus	+	+	+	+	+	-	-	-	-	-	-
Staphylococcus aureus	+	+	+	+	+	+	-	-	-	-	-

Comparison of our study with previous works

The merit of the present work has been compared to others for the synthesis of silver NPs (Table 7). According to the obtained results, our method shows

more satisfied results regarding the particle size. As shown in Table 7, using *Thymbraspicata*L causes the size of Ag NPs to be about 20 nm which is smaller than the previous methods (Table 7, Entry 10).

Table 7. comparison of present method for preparation of silver NPs using different plant extracts.

Entry	Plants extract	Size (nm)	Plant's part	Shape	References
1	Buteamonosperma bark	35	Bark Plant	Face-Centered Cubic	[27]
2	Ziziphoratenuior	8–40	Leaves	Spherical	[28]
3	Vitisvinifera	30–40	Fruit	–	[29]
4	Alternanthera dentate	50–100	Leaves	Spherical	[30]
5	Boerhaaviadiiffusa	25	Whole plant	Spherical	[31]
6	Psoraleacorylifolia	100–110	Seeds	–	[32]
7	Meliadubia	35	Leaves	Spherical	[33]
8	Ferula gumosa	30	Leaves	Spherical	[34]
9	Scropholaria Striate	22	Whole plant	Spherical & FCC	[35]
10	ThymbraspicataL	20	Whole plant	Spherical & FCC	This Study

Conclusion

In the presented study, the antimicrobial activity of *Thymbraspicata*L aqueous extract and synthesized silver NPs using

the extract on 4 bacteria and 2 fungi have been investigated. It was found that the NPs have more antimicrobial effects at proper concentrations

as compared to their own extract and silver solution. However, both the extract and the NP solutions have concentration-dependent antimicrobial activity. The resistance patterns of bacteria against the extract showed more sensitivity of gram positive bacteria as compared to the gram negative ones, so that at low concentrations (25 mg/mL), gram-negative bacteria were grown and resistant, however, by increasing concentrations (above 50 mg/mL), the growth of both groups was inhibited. Also, investigation of antifungal effects of extract showed a relatively high sensitivity of this group to this extract. In the antimicrobial effects investigation of silver NPs, these NPs showed a significant effect against all microbes, that unlike the extract, NPs had a significant inhibitory effect on gram-negative bacteria as compared to gram-positive ones. Since the extracts and silver NPs showed high antimicrobial activity, it is recommended to use them in various fields to prevent contamination and diffuse pathogens.

Acknowledgments

The authors gratefully acknowledge Islamic Azad University of Arak for financial support of this project

References

- [1] K. Govindaraju, S. Tamilselvan, V. Kiruthiga, G. Singaravelu, *J. Biopest.*, **2010**, *3*, 394-399.
- [2] A. Nanda, M. Saravanan, *Nanomed. Nanotech. Biol. Med.*, **2009**, *5*, 452-456.
- [3] (a) M. Gajbhiye, J. Kesharwani, A. Ingle, A. Gade, M. Rai, *Nanomed. Nanotech. Biol. Med.*, **2009**, *5*, 382-386; (b) A.R. Shahverdi, S. Minaeian, H.R. Shahverdi, H. Jamalifar, A.-A. Nohi, *Proc. Biochem.*, **2007**, *42*, 919-923.
- [4] (a) N. Ahmad, S. Sharma, M. K. Alam, V. Singh, S. Shamsi, B. Mehta, A. Fatma, *Coll. Surf. Bio.*, **2010**, *81*, 81-86; (b) S. Sajjadifar, *Chemical Methodologies*, **2017**, *1*, 1-11; (c) S. Rezaayati, S. Sajjadifar, *Journal of Sciences, Islamic Republic of Iran*, **2014**, *25*, 329-337; (d) H. Veisi, D. Kordestani, S. Sajjadifar, M. Hamelian, *Iran. Chem. Commun.*, **2014**, *2*, 27-33
- [5] F. Okafor, A. Janen, T. Kukhtareva, V. Edwards, M. Curley, *Int. J. Environ. Res. Public Health*, **2013**, *10*, 5221-5238.
- [6] (a) Z. Zhanjiang, L. Jinpei, *Rare Met. Mater. Eng.*, **2012**, *41*, 1700-1705; (b) C. Jianrong, M. Yuqing, H. Nongyue, W. Xiaohua, L. Sijiao, *Biotech. Adv.*, **2004**, *22*, 505-518.
- [7] (a) K. Chaloupka, Y. Malam, A. M. Seifalian, *Trends Biotechnol.*, **2010**, *28*, 580-588; (b) N. Kulkarni, U. Muddapur, *J. Nanotechnol.*, **2014**, 2014. <http://dx.doi.org/10.1155/2014/510246>
- [8] S. Ankanna, T. Prasad, E. Elumalai, N. Savithramma, *Dig J Nanomater Biostruct*, **2010**, *5*, 369-372.
- [9] P. Christian, F. Von der Kammer, M. Baalousha, T. Hofmann, *Ecotoxicology*, **2008**, *17*, 326-343.
- [10] (a) C. Marambio-Jones, E. M. Hoek, *J. Nanopart. Res.*, **2010**, *12*, 1531-1551; (b) S. Sajjadifar, H. Vahedi, A. Massoudi, O. Louie, *Molecules*, **2010**, *15*, 2491-2498; (c) S. Sajjadifar, Z. Arzehgar, A. Ghayuri, *Journal of the Chinese Chemical Society*, **2018**, *65*, 205-211; (d) S. Sajjadifar, O. Louie, *Journal of chemistry*, **2013**, 2013, <http://dx.doi.org/10.1155/2013/674946>; (e) S. Sajjadifar, G. Mansouri, S. Miraninezhad, *Asian J. Nanosci. Mater.*, **2018**, *1*, 11-18.
- [11] (a) M. Khodaie, N. Ghasemi, M. Ramezani, *Iran. Chem. Commun.* **2019**, 502-513; (b) M.A. Nasser, M. Shahabi, A. Allahresani, M. Kazemnejadi, *Asian J. Green Chem.*, **2019**, *3*, 382-390.
- [12] (a) J.L. Gardea-Torresdey, E. Gomez, J.R. Peralta-Videa, J.G.

- Parsons, H. Troiani, M. Jose-Yacaman, *Langmuir*, **2003**, *19*, 1357-1361; (b) A. D. Dwivedi, K. Gopal, *Colloids Surf. A*, **2010**, *369*, 27-33.
- [13] (a) S. Irvani, B. Zolfaghari, *Bio Med Res. Int.*, **2013**, *2013*; (b) G. Von White, P. Kerscher, R.M. Brown, J. D. Morella, W. McAllister, D. Dean, C. L. Kitchens, *J. Nanomater.*, **2012**, *2012*, <http://dx.doi.org/10.1155/2012/730746>; (c) E. Rezaee Nezhad, F. Heidarizadeh, S. Sajjadifar, Z. Abbasi, *Journal of Petroleum Engineering*, **2013**, *2013*, <http://dx.doi.org/10.1155/2013/203036>; (d) S. Sajjadifar, *International Journal of ChemTech Research*, **2013**, *5*, 385-389; (e) M.A. Zolfigol, H. Vahedi, A. Massoudi, S. Sajjadifar, O. Louie, *Clinical Biochemistry*, **2011**, *13*, S219.
- [14] (a) M. Zhang, K. Zhang, B. De Gusseme, W. Verstraete, R. Field, *Biofouling*, **2014**, *30*, 347-357; (b) V. Gopinath, D. MubarakAli, S. Priyadarshini, N.M. Priyadharsshini, N. Thajuddin, P. Velusamy, *Colloid. Surf. Bio.*, **2012**, *96*, 69-74.
- [15] (a) S.K. Das, M.M.R. Khan, A. K. Guha, A.R. Das, A.B. Mandal, *Bioresource Technol.* **2012**, *124*, 495-499; (b) M.M. Khalil, E.H. Ismail, K.Z. El-Baghdady, D. Mohamed, *Arab. J. Chem.* **2014**, *7*, 1131-1139.
- [16] S. Perni, V. Hakala, P. Prokopovich, *Colloid. Surf. A.*, **2014**, *460*, 219-224.
- [17] (a) A.S. Dehnavi, A. Raisi, A. Aroujalian, *Inorg. Nano-Met. Chem.* **2013**, *43*, 543-551; (b) H. Veisi, A. Sedrpoushan, P. Mohammadi, A.R. Faraji, S. Sajjadifar, *RSC Advances*, **2014**, *4*, 25898-25903; (c) S. Sajjadifar, M.A. Zolfigol, G. Chehardoli, S. Miri, *International Journal of ChemTech Research*, **2013**, *5*, 422-429; (d) E. Rezaee Nezhad, S. Sajjadifar, Z. Abbasi, S. Rezayati, *Journal of Sciences, Islamic Republic of Iran*, **2014**, *25*, 127-134.
- [18] A. Riesenber, H. Kaspar, A. T. Feßler, C. Werckenthin, S. Schwarz, *Vet. Microbiol.*, **2016**, *194*, 30-35.
- [19] F. Rad, F. Aala, N. Reshadmanesh, R. Yaghmaie, *Ind. J. Dermatology*, **2008**, *53*, 115v.
- [20] A. Morshedi, M. Dashti-R, M. Dehghan-H, M. Bagherinasab, A. Salami, *J. Med. Plant.*, **2011**, *4*, 48-57.
- [21] M. Negahban, S. Moharramipour, F. Sefidkon, *J. Asia-Pac. Entomol.*, **2006**, *9*, 61-66.
- [22] X.-F. Zhang, Z.-G. Liu, W. Shen, S. Gurunathan, *Int. J. Mol. Sci.* **2016**, *17*, <https://doi.org/10.3390/ijms17091534>.
- [23] H.J. Lee, J.Y. Song, B.S. Kim, *J. Chem. Technol. Biotechnol.* **2013**, *88*, 1971-1977.
- [24] Y. Wang, X. He, K. Wang, X. Zhang, W. Tan, *Colloid. Surf. B.*, **2009**, *73*, 75-79.
- [25] P. Magudapathy, P. Gangopadhyay, B. Panigrahi, K. Nair, S. Dhara, *Physica B: Condensed Matter* **2001**, *299*, 142-146.
- [26] (a) R. Sithara, P. Selvakumar, C. Arun, S. Anandan, P. Sivashanmugam, *J. Adv. Res.* **2017**, *8*, 561-568; (b) S. Sajjadifar, S. Rezayati, *International Journal of ChemTech Research*, **2013**, *5*, 1964-1968
- [27] S. Pattanayak, M.M.R. Mollick, D. Maity, S. Chakraborty, S.K. Dash, S. Chattopadhyay, S. Roy, D. Chattopadhyay, M. Chakraborty, *J. Saudi. Chem. Soc.*, **2017**, *21*, 673-684.
- [28] B. Ulug, M.H. Turkdemir, A. Cicek, A. Mete, *Spectrochim. Acta A.*, **2015**, *135*, 153-161.
- [29] G. Gnanajobitha, K. Paulkumar, M. Vanaja, S. Rajeshkumar, C. Malarkodi, G. Annadurai, C. Kannan, *J. Nanostructure Chem.* **2013**, *3*, <https://doi.org/10.1186/2193-8865-3-67>.
- [30] D.A. Kumar, V. Palanichamy, S. M. Roopan, *Spectrochim. Acta A.*, **2014**, *127*, 168-171.

[31] Q. Sun, X. Cai, J. Li, M. Zheng, Z. Chen, C.-P. Yu, *Colloid Surf. A: Physicochem. Eng. Aspects.*, **2014**, *444*, 226-231.

[32] D. Sunita, D. Tambhale, V. Parag, A. Adhyapak, *Int. J. Pharm. Biol. Sci.*, **2014**, *5*, 457-467.

[33] V. Kathiravan, S. Ravi, S. Ashokkumar, *Spectrochim. Acta A.*, **2014**, *130*, 116-121.

[34] F. Mohammadi, M. Yousefi, R. Ghahremanzadeh, *Adv. J. Chem. A.*, **2019**, *2*, 266-275. DOI: 10.33945/SAMI/AJCA.2019.4.1

How to cite this manuscript: Tayeb AB Matin, Nahid Ghasemi, Keivan Ghodrati, Majid Ramezani. "Biosynthesis and characterization of silver nanoparticles: A *Thymbra spicata*L extract approach and study their antibacterial and antifungal activity". *Eurasian Chemical Communications*, 2019, 527-544.